

Advanced Physical Inspection Methods for Counterfeit IC Detection

Sina Shahbazmohamadi, and Domenic Forte, and Mark Tehranipoor

Center for Hardware Assurance, Security, and Engineering (CHASE)

University of Connecticut, Storrs, CT, USA

Email: {sina, forte, tehrani}@engr.uconn.edu

Introduction

The remarkable increase in counterfeit parts (a factor of 4 since 2009) [1] is a huge reliability and security concern in various industries ranging from automotive electronics to sensitive military applications increasing the possibility of premature failure in critical systems [2-5]. Counterfeit parts can also incur a great financial loss to legitimate electronics companies [6]. The issue is even more alarming as the counterfeiters use more sophisticated methods making counterfeit detection a much harder task [7-8]. Therefore, it is reasonable to develop more advanced counterfeit detection methods targeting a more efficient detection of sophisticated counterfeited parts.

Possible methods for counterfeit electronic parts detection can be classified into two main categories: physical inspection and electrical testing [3, 5, 9, and 10]. The physical inspection techniques can potentially be extended to different integrated circuit (IC) types (analog, digital, mixed-signal, FPGAs, and memories.). However there are some challenges: First, there is no specific equipment or test technique that can target all the defects associated with counterfeit ICs. Previous efforts have shown the possibility of more than 60 [9-10] different exterior, interior and compositional defect types making it difficult for any single instrument to detect all. Therefore, one has to resort to utilizing different instruments ranging from optical microscopes to high-tech Scanning and Transmission electron microscopes (SEMS and TEMs) making physical detection a costly and time-consuming process. Second, most methods require a subject matter expert (SME) to interpret the test results which in turn leads to additional cost, inefficiency and inconsistency and prevents us from automating the process. Third, the issue associated with physical inspections is the destructive nature of most tests. Having access to the interior features is inevitable for complete counterfeit detection tests which usually entails decapsulation of the part, which is inherently destructive method. The common practice for detecting remarked and black-top coated parts is also based on chemical or mechanical destructive tests. In terms of using microscopy and spectroscopy techniques, one has to do the imaging and analysis on various locations which entails multiple sessions of imaging which further adds to the cost and time in addition to the likelihood of damaging the chip while handling. Finally, counterfeit detection usually requires having a known authentic sample (commonly referred to as the “golden IC”) for comparison. This can raise issues where such a golden IC may not exist or difficult to be obtained.

The major contribution of this paper is to tackle these issues by introducing and optimizing two novel three and four dimensional imaging techniques that can provide us with the necessary information on interior and exterior geometry along with the material composition for the parts under test: Four-Dimensional Scanning Electron Microscopy and Dual Energy 3D X-ray Microscopy. It will be shown that by applying the proposed modifications, we can successfully detect all the defects associated with different counterfeit parts through a single-imaging session. This could significantly reduce the cost and time of implementing physical inspections. The proposed methods are also totally non-destructive, causing no damage to the part under test while successfully detecting the interior defects. Finally, the presence of quantitative results as opposed to qualitative images can potentially eliminate the need of the SMEs’ interpretation and expertise which can further reduce the associated cost and improve the detection accuracy.

In this study, we have utilized advanced image processing and image analysis tools to establish a more consistent and accurate image perception. In particular, we tackle the issue of texture characterization. Improper texture and/or texture inconsistency are deemed a defect often present in counterfeit parts, but quantifying it in such way that one can distinguish between the counterfeit and authentic parts, is a major challenge. Also, optical methods can potentially misrepresent texture variations due to light intensity and exposure which can bias the detection process. By using multiple surface parameters to quantify texture variation, we have been able to distinguish more sophisticated blacktop-coated samples and sanding issues, two of the most common phenomena in counterfeit ICs. We also use inconsistencies within the samples and their defects as an alternative to having a golden IC. However, the final decision has further been validated using results from 5 known authentic samples.

Background

Counterfeit parts are classified into 7 main categories: Recycled, remarked, overproduced, defective, forged documentation and tampered [2]-[5]. A detailed explanation of each can be found in [2].

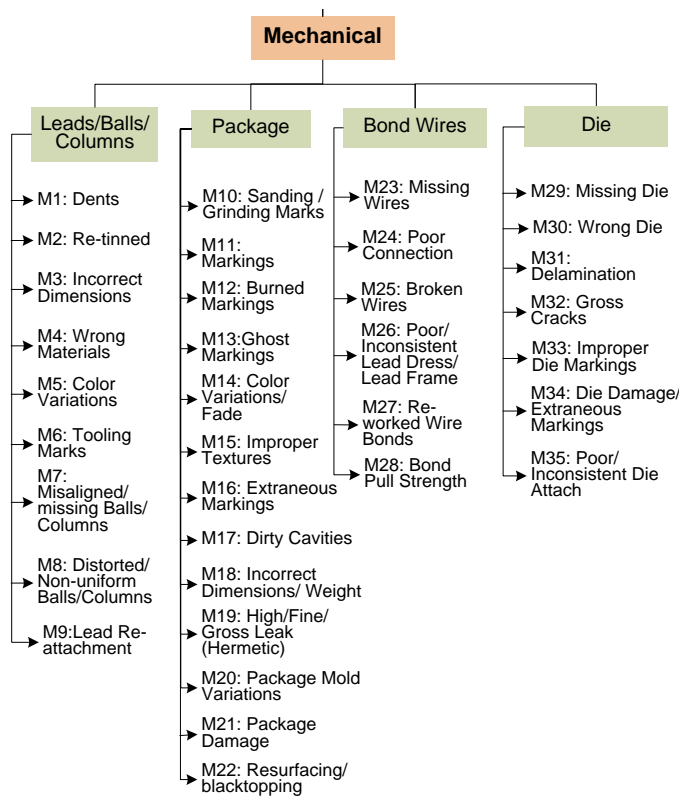


Figure 1(a) Taxonomy of Mechanical Defects

The mechanical defects that are associated with these counterfeit types can be seen in Fig. 1(a) which is the target of physical inspection methods. The defects include both geometric abnormalities and compositional discrepancies and inconsistencies. Such variety of defects demands utilization of various test methods as shown in Fig. 1(b) which demand more than 19 instruments. It must be noted that some of these defects are also associated with quality issues.

Preliminaries

Five Intel flash memory ICs have been analyzed for counterfeit detection without prior knowledge of them being counterfeit or authentic. Sample image of the chip using a VHX2000 Keyence digital microscope (Itasca, IL) has been provided in Fig. 2.

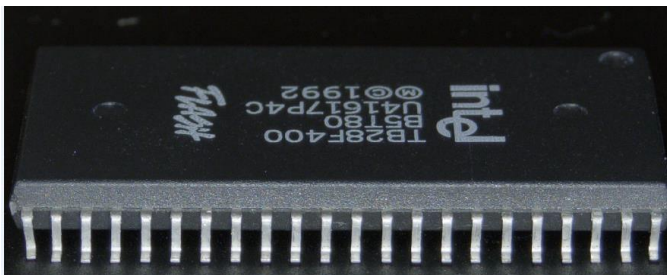


Figure 2- Sample Digital Microscope Image of the ICs investigated

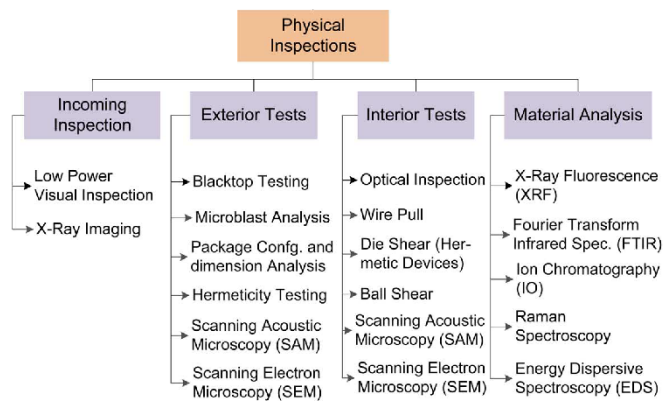


Figure 1(b) - Physical inspection methods

After acquiring digital microscope images of all chips using the cited instrument, the samples have been investigated by Scanning Electron Microscopy (SEM) and X-ray Microscopy. SEM analyses have been performed using FEI Quanta 250 under low vacuum mode with no sample preparation. Energy dispersive Spectroscopy (EDS) was performed in the same imaging session using an X-ray detector and EDAX software. Images were taken at three tilt angles using eucentric tilting at the working distance in order to perform stereo photogrammetry for 3D surface geometry reconstruction and further texture analysis. XRM analysis was performed using Xradia Versa 510 (Pleasanton, CA) using large field of view (LFOV) and 4X magnification objectives.

Proposed Method

4-Dimensional Scanning Electron Microscopy (SEM)

SEMs are extensively used in counterfeit detection as a defect characterization tool. SEM micrographs have been qualitatively used to characterize the surface and /or texture of the electronic parts. The large depth of field of SEM makes it a much more appropriate tool for texture inconsistency analysis comparing to optical microscope [11]. However, SEM images remain to be two-dimensional lacking quantified depth information.

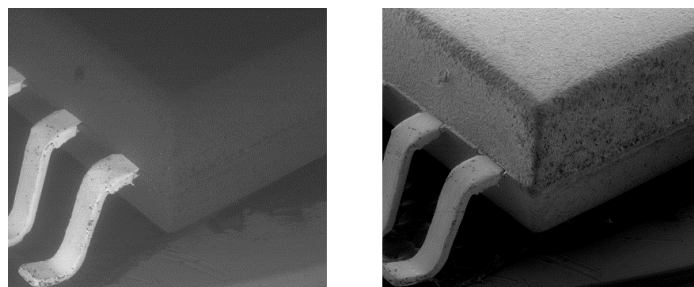


Figure 3- Two images of the exact same location of the same IC with different imaging parameters

Texture variation is not always readily seen using microscopy techniques. Figure 3 shows two SEM images of the exact

same location acquired by different acquisition parameters. As it can be seen the variation in the texture is almost entirely invisible while it can be easily recognized in the left image. Another issue is such images always require an SME to interpret the data as it lacks quantified information and is not suitable for automation.

In order to obtain 3D images of the surface of the inspected ICs, we have used stereo-photogrammetry, a well-established technique in aerial imaging which has been developed with SEM for 3D reconstruction. This technique consists of 3 stages: [12]

- 1) *Image Acquisition*: Taking images of the same area from different perspectives.
- 2) *Matching Algorithm*: A computer algorithm to find homologue points, i.e. points belonging to the same location
- 3) *Extracting depth information*; Using projective geometry and Piazzesi Algorithm [8] to find three dimensional coordinates and reconstruct digital elevation model (DEM)

Figures 4(a) and (b) demonstrate the acquired images on a dimple (mold cavity) of the ICs taken at two tilting angles of positive and negative ten degrees. The working distance and the angle have been optimized using guidelines elaborated in reference [12]. Figure 4(c) shows the 3D reconstructed image with the color map corresponding to height values.

In order to extend the information to the 4th dimension, EDS mapping has been used on the exact same area and the images are reconstructed in color to show any variations in material composition. Figure 5 demonstrates a similar image to that of Fig. 4 (a) and (b) in terms of location, however in this figure color represents material composition and shows the presence of different material on the wall of the dimple.

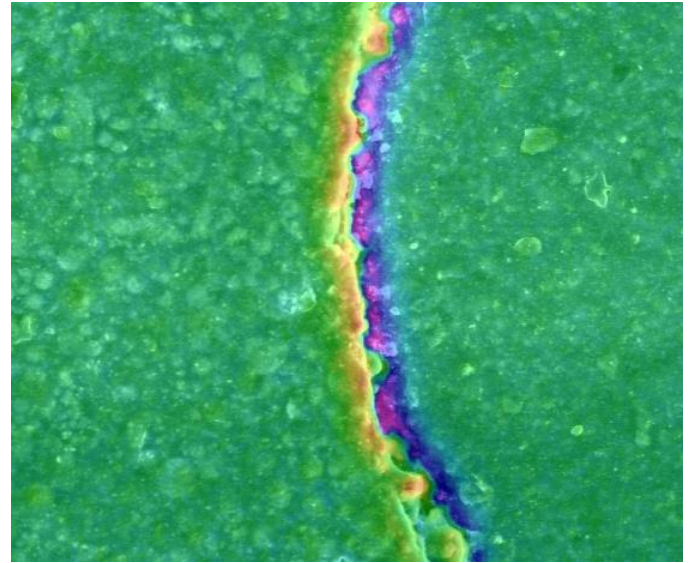


Figure 5 Compositional Map on the Dimple, where green represents Carbon and blue, red and yellow are Si, Ti and V respectively

Presence of inorganic materials on the package of these chips is an anomaly. Further analysis has shown the same material composition, that is (Ti and V), on the markings of the chip. The presence of Si in the image is also an indication of sanding. This analysis can help us to not only distinguish the defect but also find out the process of counterfeiting which can contribute to further counterfeit detection and prevention. In this case, it appears that the previous marking on the chip has been removed using SiC paper sanding and then remarked. Combining Fig. 4(c) and 5 can provide us with four dimensional information on the sample which can greatly facilitate the counterfeit detection. This is shown in Fig. 6.

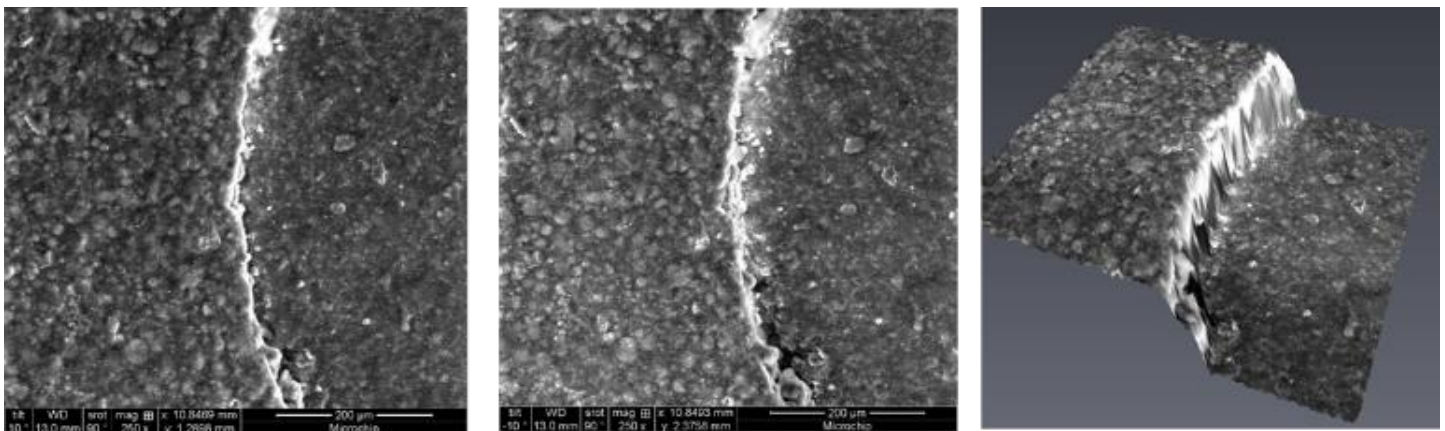


Figure 4 Tilted (a) and (b) and reconstructed 3D (c) images

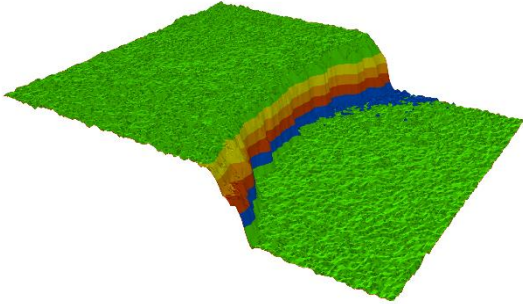


Figure 6- four-dimensional image of a Dimple, with colors represent sample material as Fig. 5.

Dual Energy 3D X-ray Microscopy

2D radiological X-rays is a well-established technique to examine the interior attributes of the chip without decapsulation.[14] By taking multiple 2D X-ray projections and then reconstructing them, one can obtain the three dimensional information of the interior and the exterior image of the imaged object. This technique is commonly known as X-ray Tomography scan. Researches have used the 3D X-ray Tomography for studying electronic parts, however there have always been some issues: [15], [16]

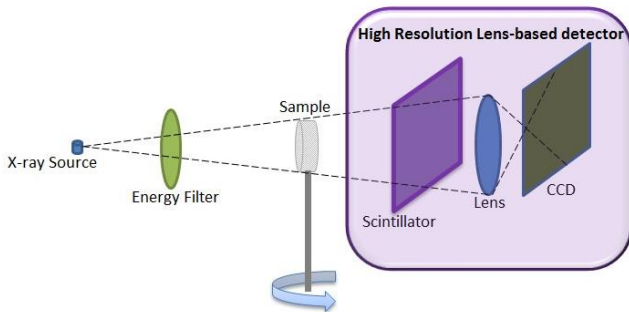


Figure 7 Schematic of the X-ray Microscope structure

1. Many electronic parts and in this particular case, the flash memory chips have high aspect ratio, which result in the obligation to have a sufficiently large working distance during tomography to avoid collision of the sample with the source and detector. However, conventional CT loses resolution significantly as the distance to the source is increased. The number of X-ray counts also decrease greatly resulting in a much worse signal to noise ratio.
2. In many cases such as the ICs studied in this work, samples are made of materials with radically different X-ray absorption coefficients. For example, the package is commonly made out of Carbon with a very low X-ray attenuation coefficient while the leads are made of Tin (Sn) which is a metal with a much higher attenuation coefficient. This entails problems associated with choosing the right X-ray source energy.

3. The process of tomography is believed to be time consuming and inefficient for everyday counterfeit detection application.

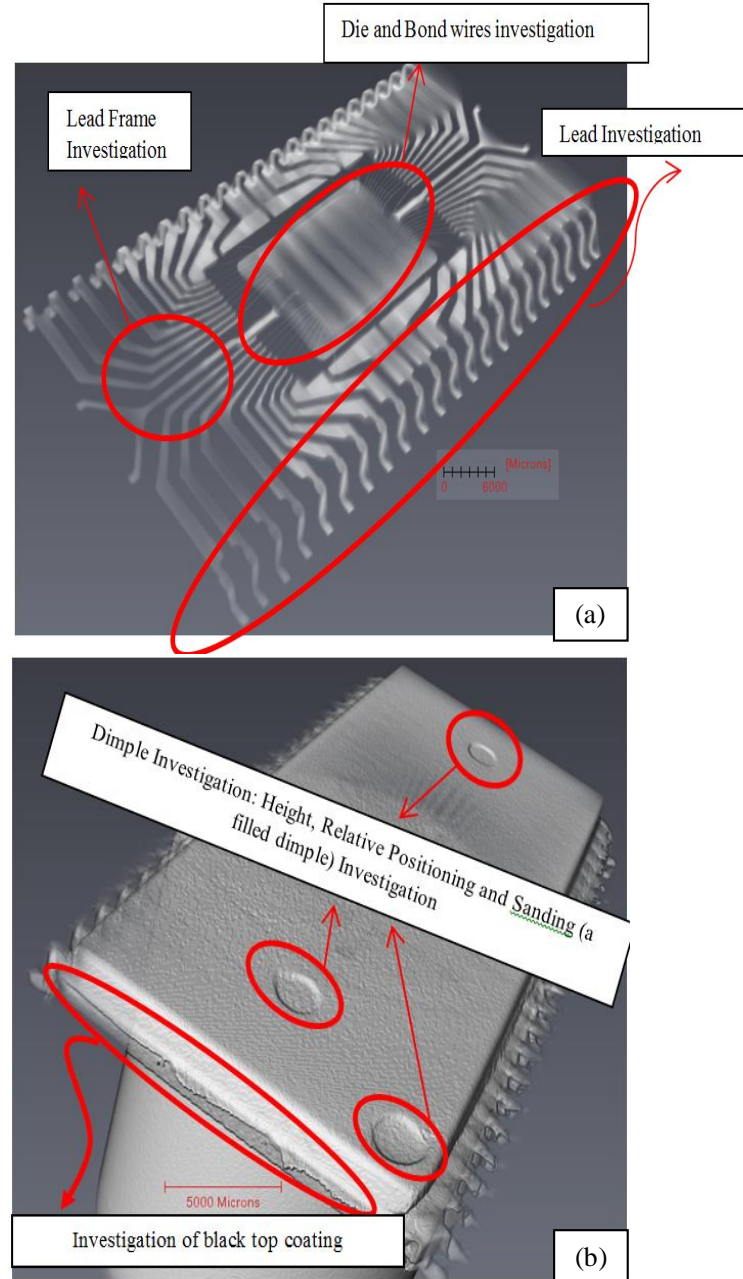


Figure 8- XCT images of ICs using low (bottom) and High (top) energy

In order to overcome these challenges, two tomographies have been performed at two different energy levels focusing on the package for the low energy ones and investigating leads with a higher energy. Use of dual energy can help us to identify both exterior and interior defects. Also the cited X-ray Microscope's architecture and use of a scintillator allows a much better resolution to be achieved at higher working distances. Figure 7 provides a schematic of the X-ray

microscopy with Resolution at a distance (Raad) propriety capability.

Also to capture the most defects in a single imaging session, the large field of view detector has been used where the entire sample can be imaged at once. Figure 8 shows a sample 3D rendered image at both high (a) and low (b) energies and the investigations that have been facilitated using the proposed technique.

Results and Discussion

Texture analysis

The data density and three dimensional information associated with 3D SEM allows performing a more detailed texture analysis. Table 1 shows the surface parameters that are extracted from the surface of the chips to quantitatively address inconsistencies. In the table, “Z” denotes the height information that can be extracted through the entire rectangular surface with the length M and width N.

Table 1- Surface Parameters for Texture Analysis

Parameter	Definition	Formulation
Sa: Average Roughness	Arithmetic mean of absolute height values of the area	$\frac{1}{MN} \sum_{\substack{1 \leq i \leq M \\ 1 \leq j \leq N}} Z(i, j)$
Sq: RMS Roughness	Root mean square value of the height of the area	$\frac{1}{MN} \sum_{\substack{1 \leq i \leq M \\ 1 \leq j \leq N}} Z^2(i, j)$
Sp: Peak	Largest Height of the area	$\max_{\substack{1 \leq i \leq M \\ 1 < j < N}} Z(i, j)$
Sv: Valley	Minimum Height of the area	$\min_{\substack{1 \leq i \leq M \\ 1 < j < N}} Z(i, j)$
Sku: Peakedness	Kurtosis of the area	$\frac{1}{MNSq^4} \sum_{\substack{1 \leq i \leq M \\ 1 \leq j \leq N}} Z^4(i, j)$

Roughness parameters such as Average and RMS allow us to have a better understanding of texture variations. Height parameters can help us analyze the dimple height variations independent of the reference plane and finally kurtosis, as a measure of pointiness of the surface allows us to find sanding marks and removed markings based on the texture information. Figure 9 shows the surface parameters extracted from the 5 ICs showing that using any single parameter alone cannot show the discrepancy among the surfaces however as more surface parameters are used. The inconsistencies among the samples are better identified.

It can be seen at roughness level (Sa and Sq), only sample 5 is showing major discrepancy. Moving to height information we can see that sample 1 and sample 3 share different values than those of 2 and 4. This takes us to our fifth measure, Kurtosis

which has been kept out the Fig. 9 for scaling issues. The kurtosis values for the 5 samples are 0.98, 1.5131, 1.3048, 1.5461, and 1.358.

This suggests that the value is substantially lower for sample 1 which can be attributed to sanding. The 4-dimensional image shown in Fig. 6 also showed sanding residual materials which can further prove the process of counterfeiting.

Such characterization allows us to quantitatively prove sanding which can facilitate the process of automation. In addition, as only inconsistencies within the 5 samples are used for detection, the analysis does not require a “golden IC”. However, we have included the information about the authentic samples for validation purposes. As one can determine:

- 1) Whether such variations also appear different authentic samples
- 2) Whether the samples have different surface parameter values than the golden IC.

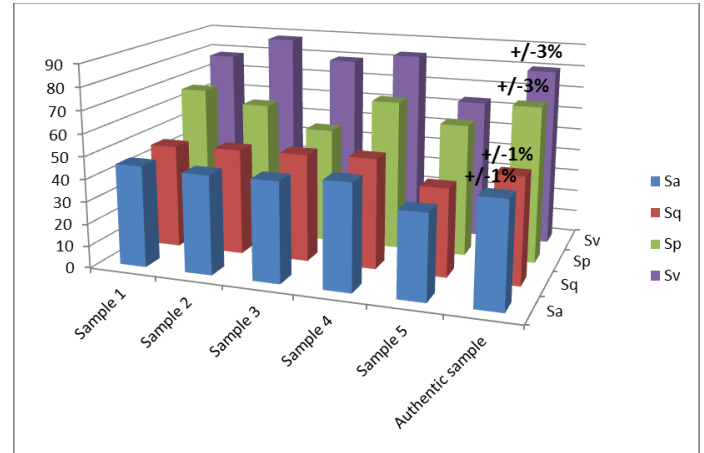


Figure 9- Surface parameters extracted from a dimple for the 5 samples in study (all values are in microns)

The authentic sample bars in Fig. 9 have a number above them showing their variations among 5 samples in percent. It is clear that the variations between the authentic samples are much smaller than that seen among the 5 studied ICs. Also we can see roughness parameters are less effective measure comparing to height parameters and Kurtosis values.

Additional texture analysis using 3D SEM data is calculated by the areal autocorrelation function (AACF) of the surface to obtain the texture directionality: [12]-[15]

$$R(t_i, t_j) = \frac{1}{(M-i)(N-j)} \sum_{l=1}^{N-j} \sum_{k=l}^{M-i} Z(x_k, y_l) Z(x_{k+i}, y_{l+j}) \quad (1)$$

$$i = 0, 1, \dots, m < M; j = 0, 1, \dots, n < N; t_i = i \cdot \Delta x; t_j = j \cdot \Delta y$$

Figure 10 shows the AACF of each of the surfaces where the value of autocorrelation ranges from -1 (no correlation in pink) to 1 (maximum correlation in red). Additional information on AACF can be found in references [17-22]

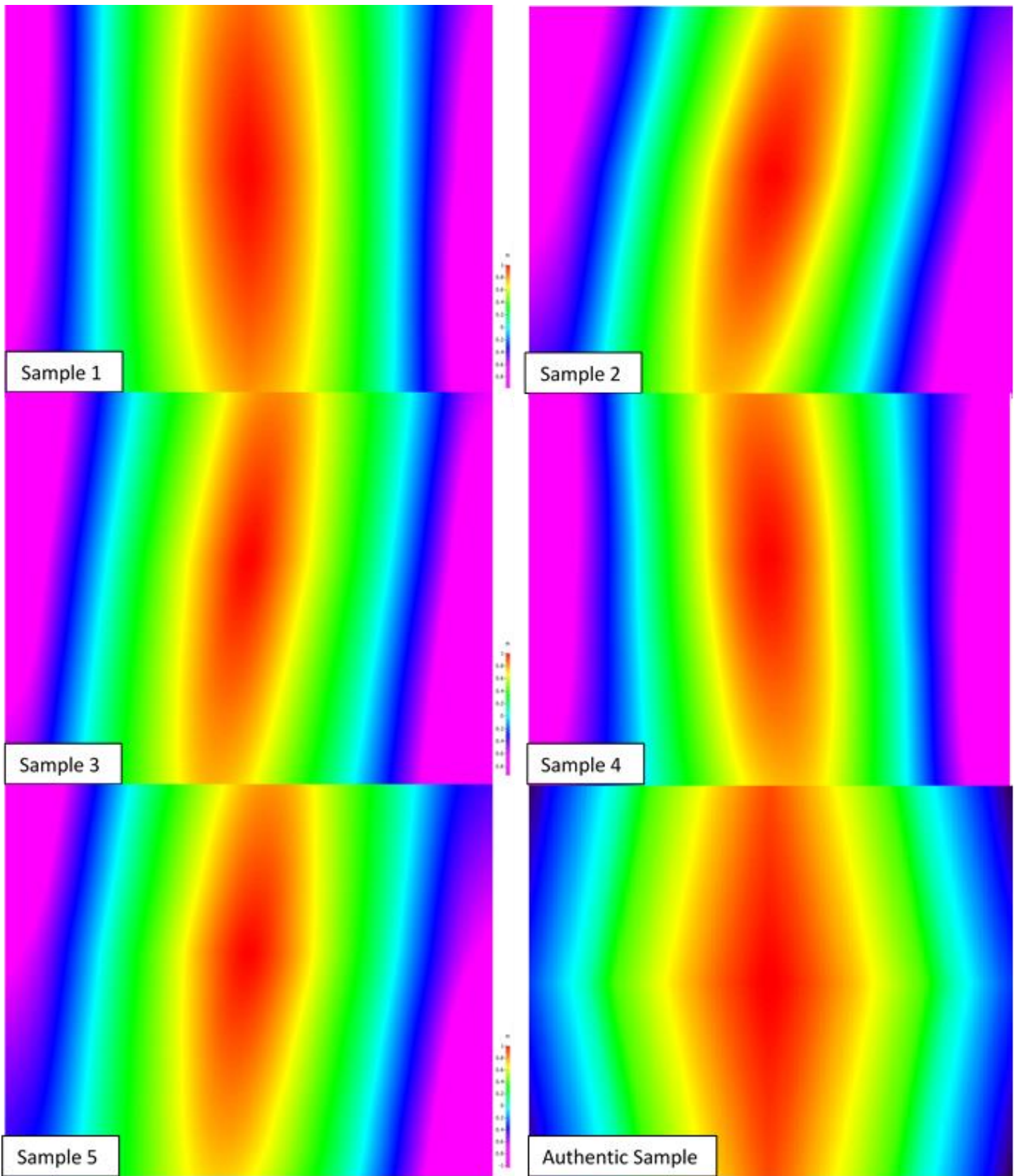


Figure 10-AACF of all samples showing different texture direction

The ideal uniform direction in sample 1 also proves the sanding case. In addition further discrepancies were recorded between samples that initially had relatively similar roughness parameters.

To further investigate if similar cases can be identified in authentic samples, similar studies were conducted on 5 authentic samples. All figures and exact values have been excluded for brevity and only one has been shown in Fig. 10 as an example. All the authentic samples shared a similar ACCF. This further proves that discrepancies in the AACF can be used as another quantitative metric for counterfeit detection.

3D X-ray Results

2D X-rays can help distinguishing defects such as a wrong die/ wrong die orientation. Such study is shown for all chips in Fig. 11. It can be seen that sample 3 has a totally different die which has a different orientation and size. The other 4 samples look very similar and even comparing to the authentic sample doesn't yield conclusive evidence though it does show a small difference in bond wire patterning. This study proves that extending the information to the third dimension is inevitable

Figure 12 shows 3D images of samples 1 and 2 where one can see signs of die face delamination on sample 1 (top left) and

not in 2 (top right). Additional investigation of virtual slices shows clear images of the die face delamination in all corners. (Bottom left and right). The die face delamination can be the result of recycling and is a great reliability concern. After hours of operation, such delamination can grow to the point of breaking the bond wires. Similar images revealed same results for sample 5.

Results Summary

Combining the results from the two techniques, we have been able to identify all the 5 ICs as counterfeits. Results were discussed and confirmed with our SMEs at Honeywell who performed all the tests on the parts and obtained similar information.

All the defects identified using the techniques described are summarized in Table 2. Other common techniques or instruments utilized for detection of such defects are also provided in the last column. It can be seen that using our proposed technique can successfully detect all defects nondestructively.

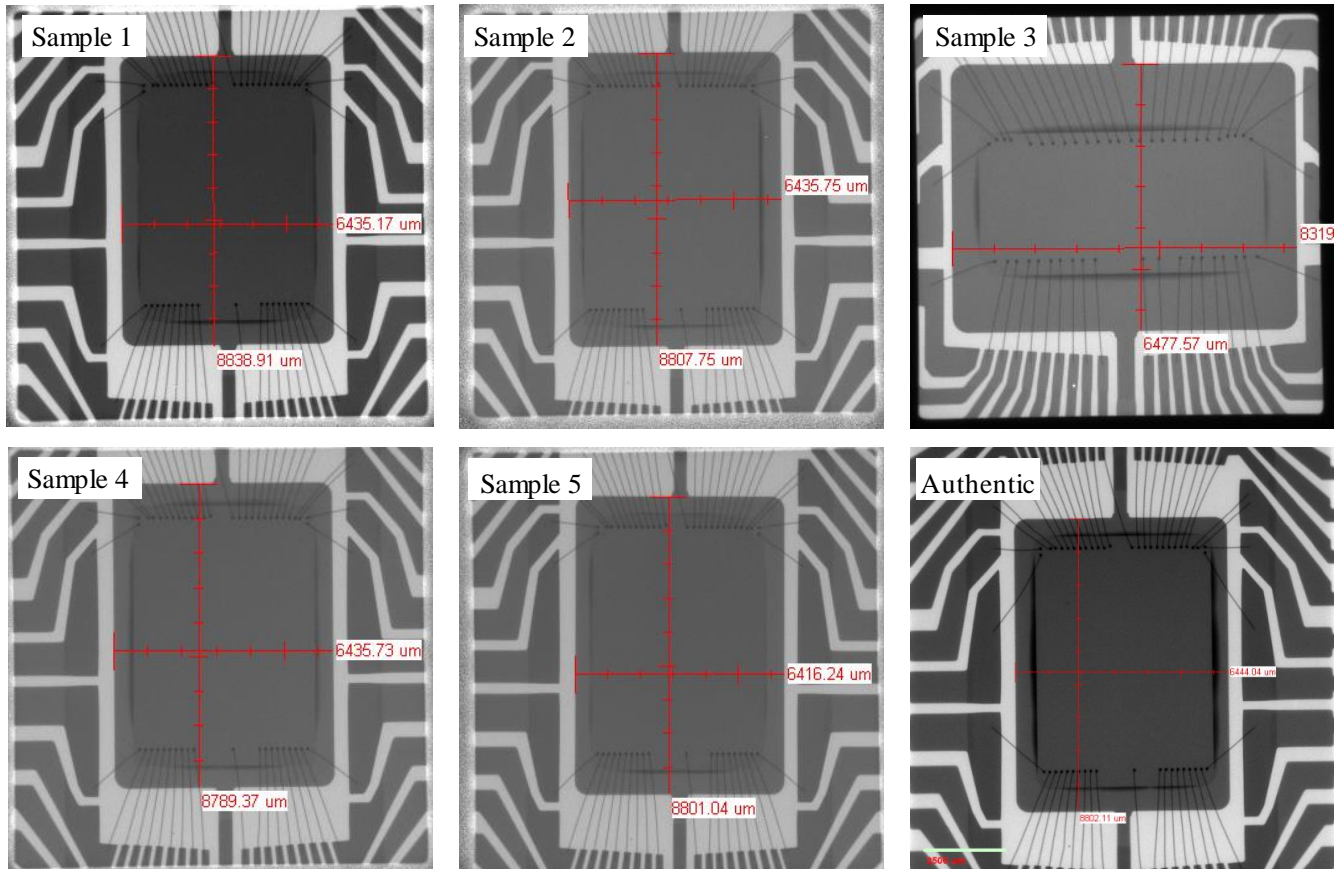


Figure 11- 2D X-rays of samples

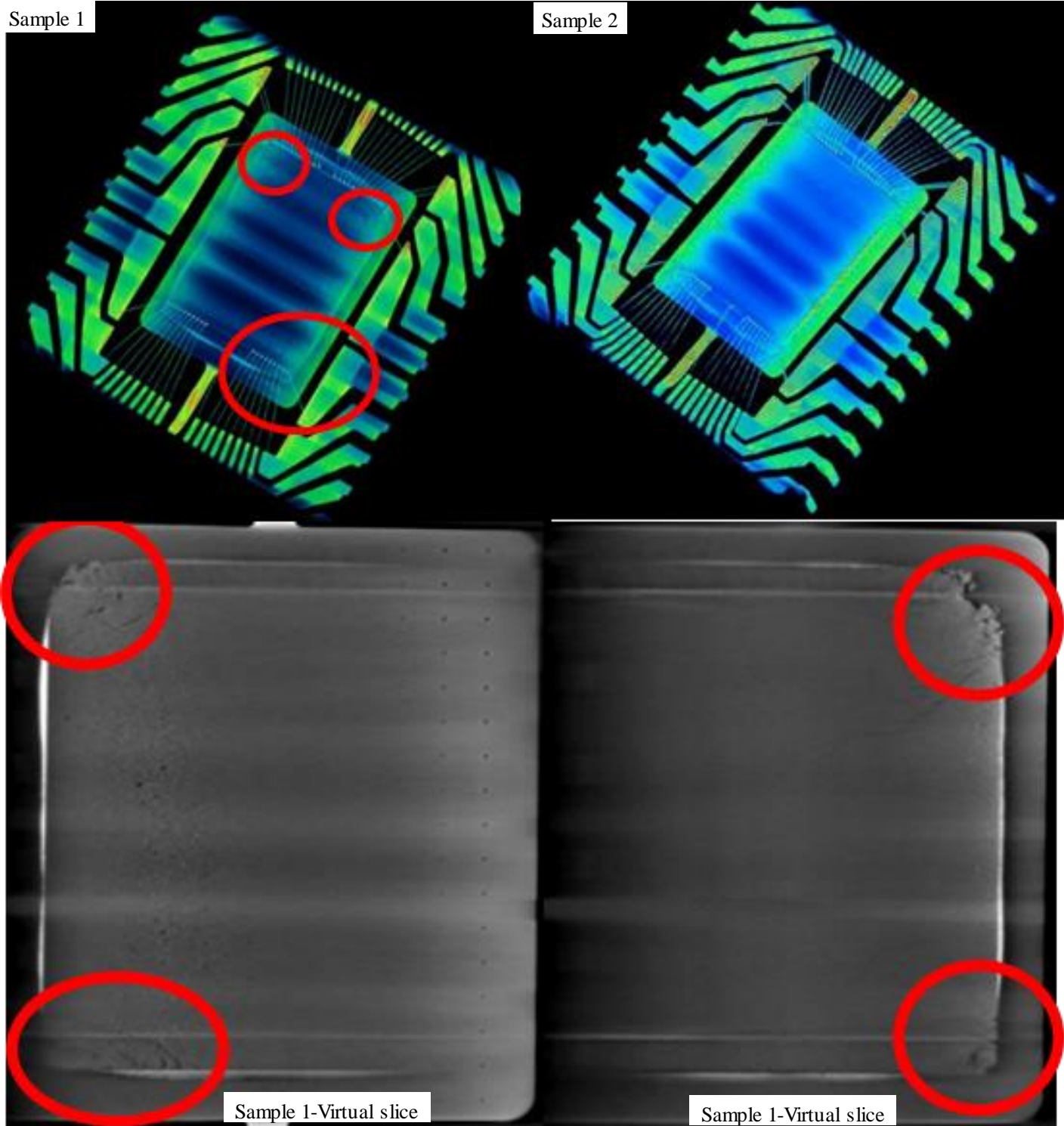


Figure 12- Top: 3D images of the die in samples 1 and 2- Showing die face delamination in sample 1
Bottom: Virtual 2D slices of sample 1 illustrating die face delamination in all corners

OBSERVATION	INSTRUMENT	OTHER COMMON METHODS
Residue on leads	SEM/X-ray	X-ray Fluorescence (XRF), Optical Microscopy
Sanding marks	SEM/EDS	Optical Microscopy, XRF
Coated/filled dimples	SEM/X-ray	LSM, Optical profilometry
Dimple depth variation	SEM/X-ray	LSM, Optical Profilometry
Incorrect lead plating (Sn vs. Sn/Pb)	SEM/EDS	XRF
No exposed lead base metal	SEM	XRF, Optical Methods
Bent leads	SEM/X-ray	Optical Methods
Metal shavings and/or tin whiskers on leads	SEM	SEM, Optical Microscopy
Different die sizes	X-ray	Decapsulation, Scanning Acoustic Microscopy (SAM)
Different lead frames	X-ray	Decapsulation
Wire bond pattern variations	X-ray	Decapsulation, SAM
No barrier metal under pure Sn lead finish	SEM	XRF, Optical Microscopy
Blacktopping (top and bottom surfaces)	SEM/X-ray	Destructive Liquid Testing

Table 2 - Summary of results

Conclusions

Two novel imaging techniques have been introduced and applied as a powerful tool for detecting defects associated with counterfeit electronic parts. The techniques are entirely non-destructive and don't require any sample preparation. In addition, all information can be obtained in a single imaging session which can greatly contribute to the time and cost of counterfeit detection procedures. Quantitative analysis has also been proposed for the first time for texture analysis which has been in an issue of controversy. It has been shown that three dimensional characterization of the dimples along with compositional analysis can help us better identify counterfeit parts as well as to understand the process which can be used for further counterfeit detection and prevention purposes. The 3D X-ray analysis has also been used as an effective way to access the interior properties of the ICs and proved to be necessary in cases where 2D X-ray doesn't provide sufficient geometry. It has been shown the observed defects in counterfeit parts are not present in the authentic samples. However, one doesn't necessarily require a so-called golden IC to check for several defects discussed in

this paper. Although the authors have taken the preliminary steps of automation in counterfeit detection by providing quantitative metrics, more work has to be done to establish a rigorous algorithm for such effort. The authors seek to develop such algorithms in their future work while improving the quality of the proposed methods. It must be noted that current study requires a more detailed statistical analysis to prove if the detection is consistent.

Acknowledgments

This work was supported in part by the National Science Foundation under grant CCF-1423282 and grants from Honeywell and the Missile Defense Agency (MDA). The authors would also like to thank Daniel DiMase and Steve Walters for providing the samples and their comments as SMEs.

References

- [1] J. Cassell, "Reports of Counterfeit Parts Quadruple Since 2009, Challenging US Defense Industry and National Security," Apr. 2012.
- [2] U. Guin, K. Huang, D. DiMase, J. M. Carulli Jr., M. Tehranipoor, and Y. Makris, "Counterfeit Integrated Circuits: A Rising Threat in the Global Semiconductor Supply Chain," Proceedings of the IEEE, 2014
- [3] U. Guin, D. DiMase, and M. Tehranipoor, "Counterfeit Integrated Circuits: Detection, Avoidance, and the Challenges Ahead," Journal of Electronic Testing: Theory and Applications (JETTA), 2014.
- [4] Guin U., D. Forte and M. Tehranipoor, "Anti-Counterfeit Techniques: From Design to Resign," Microprocessor Test and Verification (MTV), 2013.
- [5] U. Guin, M. Tehranipoor, D. DiMase and M. Megrdichian, "Counterfeit IC Detection and Challenges Ahead," ACM SIGDA, 2013.
- [6] IHS iSuppli, "Top 5 Most Counterfeited Parts Represent a \$169 Billion Potential Challenge for Global Semiconductor Market," 2011.
- [7] CHASE, "ARO/CHASE Special Workshop on Counterfeit Electronics," January 2013,
<http://www.chase.uconn.edu/aroCHASE-special-workshop-on-counterfeit-electronics.php>.
- [8] CHASE, "CHASE Workshop on Secure/Trustworthy Systems and Supply Chain Assurance," April 2014,
<https://www.chase.uconn.edu/chase-workshop-2014.php>.
- [9] U. Guin, D. DiMase, and M. Tehranipoor, "A Comprehensive Framework for Counterfeit Defect Coverage Analysis and Detection Assessment," Journal of Electronic Testing: Theory and Applications (JETTA), 2014.
- [10] U. Guin and M. Tehranipoor, "On Selection of Counterfeit IC Detection Methods," IEEE North Atlantic Test Workshop (NATW), 2013.
- [11] J. Goldstein, Scanning Electron Microscopy and X-Ray Microanalysis, Springer, 2003.
- [12] S. Shahbazmohamadi and E. H. Jordan, "Optimizing an SEM-based 3D Surface Imaging Technique for Recording Bond Coat Surface Geometry in Thermal Barrier Coatings," Measurement Science and Technology, vol. 23, no. 12, pp. 125601-125601, 2012.
- [13] Piazzesi G., "Photogrammetry with the Scanning Electron Microscope," Journal of Physics E: Scientific Instruments, vol. 6, no. 4, pp. 392-296, 1973.
- [14] "AS6171/IV (WIP) Method IV - TECHNIQUES FOR SUSPECT/COUNTERFEIT EEE PARTS DETECTION BY RADIOLOGICAL TEST METHODS - SAE International," 2014. [Online]. Available: <http://standards.sae.org/wip/as6171/iv/>.
- [15] M. Cason and R. Estrada, "Application of X-Ray Micro CT for non-destructive failure analysis and package construction characterization," in Physical and Failure Analysis of Integrated Circuits (IPFA), 2011 18th IEEE International Symposium on the, pp. 1-6, 2011.
- [16] M. Cason and R. Estrada, "Physical and Failure Analysis of Integrated Circuits (IPFA), 2011 18th IEEE International Symposium on the," 2011 18th IEEE International Symposium on the, pp. 1-6, 2011.
- [17] Dong W, Sullivan P, Stout K. 'Comprehensive Study of Parameters for Characterizations Three-dimensional Surface Topography. I', Wear 1992; 159:161-171.
- [18] Dong W, Sullivan P, Stout K. 'Comprehensive Study of Parameters for Characterizations Three-dimensional Surface Topography. II', Wear 1993; 167:9-21.
- [19] Dong W, Sullivan P, Stout K. 'Comprehensive Study of Parameters for Characterizations Three-dimensional Surface Topography. III', Wear 1994; 178:45-60.
- [20] Dong W, Sullivan P, Stout K. 'Comprehensive Study of Parameters for Characterizations Three-dimensional Surface Topography. IV'. Wear 1994; 178:29-43.
- [21] De Chiffre, Leonardo. et al. "Quantitative characterization of surface texture. "CIRP Annals-Manufacturing Technology 49.2 (2000): 635-652.
- [22] Lonardo, P. M., H. Trumpold, and Leonardo De Chiffre. "Progress in 3D surface microtopography characterization." CIRP Annals-Manufacturing Technology 45.2 (1996): 589-598.